Electronic states of perovskite-type titanium oxides located near the insulator-correlated metal boundary

1997 J. Phys.: Condens. Matter 9 3861

(http://iopscience.iop.org/0953-8984/9/19/007)

J. Phys.: Condens. Matter **9** (1997) 3861–3870. Printed in the UK PII: S0953-8984(97)81344-6

Electronic states of perovskite-type titanium oxides located near the insulator-correlated metal boundary

Masashige Onoda and Masaaki Yasumoto

Institute of Physics, University of Tsukuba, Tennodai, Tsukuba 305, Japan

Received 27 January 1997

Abstract. The electronic states of the $R\mathrm{TiO_3}$ (R = La, Ce, Pr, and Nd) perovskite system with $\mathrm{Ti^{3+}}$ ions have been explored through measurements of x-ray diffraction, transport, and magnetization. La compounds with small oxygen deficiencies, $\mathrm{LaTiO_{2.96}}$ and $\mathrm{LaTiO_{2.98}}$, have a negative temperature derivative of magnetic susceptibility at high temperatures as expected from a free-electron-like model with a large reduction of the Fermi energy. On the other hand, La compounds with excess oxygen have an anomalous positive value, suggesting the existence of a pseudogap in the density of states. The dominant contribution to transport at low temperatures of $\mathrm{LaTiO_{2.96}}$, $\mathrm{LaTiO_{2.98}}$, and $\mathrm{CeTiO_{3.00}}$ may be by extended states on account of a lack of stoichiometry and/or of a comparability of the bandwidth and the correlation energy. In $\mathrm{CeTiO_{3.00}}$, $\mathrm{PrTiO_{3.03}}$, and $\mathrm{NdTiO_{2.97}}$, the remanent magnetization at low temperatures is qualitatively understood in terms of the molecular field of the canted moment of Ti ions acting on the 4f spins of R ions.

1. Introduction

Perovskite systems with the chemical formula $R\mathrm{TiO_3}$ or $R\mathrm{VO_3}$, where R is a rare-earth element, have been studied in order to elucidate peculiar properties for the correlated 3d electrons [1–12]. Here, $\mathrm{Ti^{3+}}$ and $\mathrm{V^{3+}}$ ions of these systems have $3d^1$ and $3d^2$ configurations, respectively. The structures at room temperature are basically of $\mathrm{GdFeO_3}$ type with $a \simeq b \simeq \sqrt{2}a_c$ and $c \simeq 2a_c$, where a_c is the simple cubic perovskite dimension as applied to $\mathrm{SrTiO_3}$ with $\mathrm{Ti^{4+}}$ or $\mathrm{SrVO_3}$ with $\mathrm{V^{4+}}$.

The $R_{1-x}\mathrm{Sr}_x\mathrm{TiO_3}$ system has been considered to change from a Mott–Hubbard insulator with $x = 0$ to a band insulator with $x = 1$ as a function of x. However, in the case of $R = \mathrm{La}$, it is difficult to determine whether the stoichiometric compound with $x = 0$ is an insulator, because the bandwidth is expected to be larger than those of other compounds. As x approaches zero, the effective mass of the conduction electrons has been revealed to increase dramatically with a constant Wilson ratio of about 2 from the magnetic susceptibility and specific heat measurements [8]. Since the paramagnetic susceptibility below room temperature depends little on temperature, in spite of the large mass enhancement, the metallic phase of $R_{1-x}\mathrm{Sr}_x\mathrm{TiO_3}$ is suggested to be essentially like a Fermi-liquid. Of course, due to the large reduction of the Fermi energy, the susceptibility above room temperature may be expected to show a significant temperature dependence. Thus, the susceptibility measurement in a wide temperature region will allow us to estimate the precise Fermi energy and a band form.

Magnetic transitions exist at low temperatures in $R\mathrm{TiO_3}$. The antiferromagnetic or ferromagnetic properties come from the superexchange coupling via Ti–O–Ti linkages which

0953-8984/97/193861+10$19.50

are correlated with the ionic radii of R [3, 4]. However, an analysis of the remanence due to the magnetic transition is not complete owing to the lack of experiments.

In order to clarify the above properties, we have measured x-ray diffraction, electrical resistivity, thermoelectric power, and magnetization of the $R\mathrm{TiO_3}$ system (R = La, Ce, Pr, and Nd) that is located near the boundary between a Mott–Hubbard insulator and a correlated metal.

2. Experiments

Polycrystalline specimens of the $R\mathrm{TiO_3}$ system were prepared from a congruent melt with Ar arc furnace. Here, starting materials were $\mathrm{TiO_2}$ (99.9% purity), Ti metal (99.9% purity), $R_2\mathrm{O_3}$ (99.99% purity) for R = La and Nd, $\mathrm{CeO_2}$ (99.9% purity) for R = Ce, and $\mathrm{Pr_6O_{11}}$ (99.99% purity) for R = Pr. Thermogravimetric analysis was performed to estimate the oxygen concentration.

An x-ray powder diffraction pattern was taken with Cu Kα radiation at 290 K by a two-circle diffractometer. Electrical resistivity was measured with a DC four-terminal method in the temperature region below 300 K. Thermoelectric power was measured by a DC method below 350 K. Magnetization was taken by a Faraday method from 4.2 K to 1100 K for R = La, to 800 K for R = Ce, and to 300 K for the other compounds, where the field of up to about 8 kOe was applied. The magnetic susceptibility was estimated from the linear coefficient of magnetization against field (M–H) curve in the decreasing process of the field.

3. Results and discussion

3.1. Lattice constant and oxygen concentration

La compounds with oxygen concentrations of 2.98, 2.96, and larger than 3, hereafter called $\mathrm{LaTiO_3}$d1, $\mathrm{LaTiO_3}$d2, and $\mathrm{LaTiO_3}$e, respectively, have been prepared. The oxygen concentrations for the Ce, Pr, and Nd compounds are estimated to be 3.00, 3.03, and 2.97, respectively. Here, each accuracy to the oxygen concentration is 0.01. For these compounds, let us use the nominal composition as the compound name.

Table 1. Lattice constants of the $R\mathrm{TiO_3}$ system at 290 K.

R	a (Å)	b (Å)	c (Å)	r
La-d1	5.623(1)	5.597(1)	7.902(3)	0.996
La-d2	5.626(1)	5.600(4)	7.922(4)	0.998
La-e	5.569(4)	5.567(2)	7.875(5)	1.000
Ce	5.596(1)	—	7.858(1)	0.993
Pr	5.534(4)	5.598(4)	7.822(5)	0.994
Nd	5.520(1)	5.651(1)	7.787(1)	0.986

The lattice constants are determined as listed in table 1. Only $\mathrm{CeTiO_3}$ is tetragonal or pseudotetragonal, while the others are orthorhombic. As the ionic radius of R decreases, the volume decreases due to the tilting of $\mathrm{TiO_6}$ octahedra. These data are almost consistent with previous works [3–6]. The lattice constant ratio r defined as $r = c/\sqrt{2}a_{\mathrm{av}}$, a_{av} being the tetragonal lattice constant or the average of a and b in the orthorhombic symmetry, is found to decrease with decreasing ionic radius, except for $\mathrm{PrTiO_3}$ having excess oxygen. This

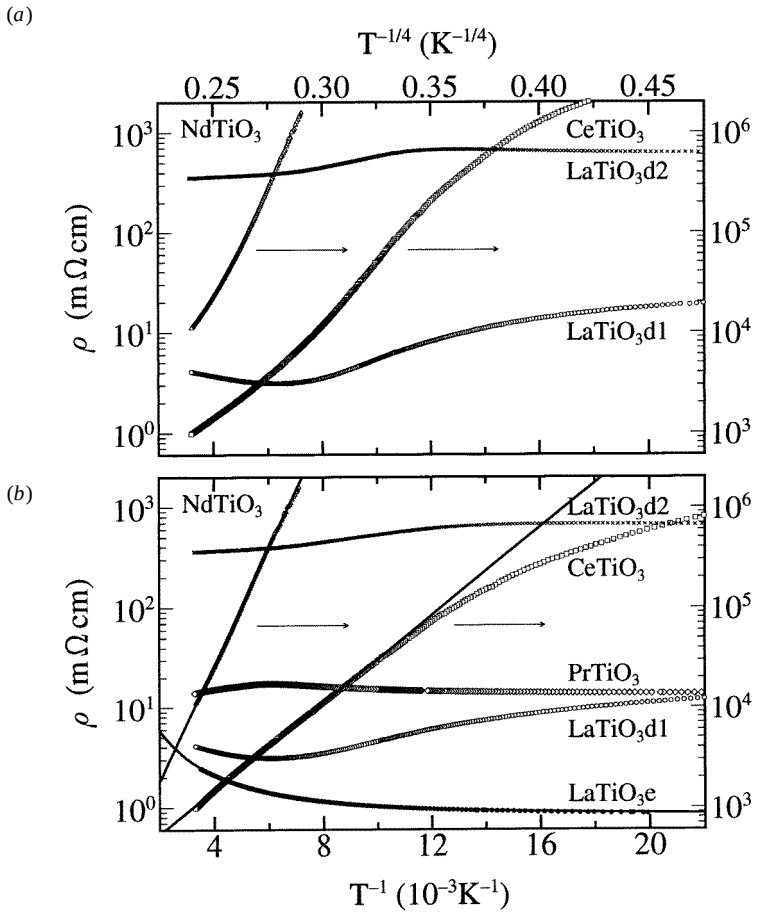

Figure 1. Temperature dependence of the electrical resistivity ρ of RTiO$_3$ with R = La, Ce, Pr, and Nd (a) log ρ against $T^{-1/4}$ and (b) log ρ against T^{-1} based on a variable-range-hopping model.

tendency has also been confirmed for the vanadium perovskites RVO$_3$ [11]. Goodenough has pointed out that this distortion, which allows the 3d^1 electron to occupy the d$_{xy}$ orbital in the dϵ state, is caused by the Jahn–Teller effect [13].

3.2. Transport properties

In figure 1(*b*), the electrical resistivity ρ of all the compounds is plotted as a function of the inverse temperature. The temperature dependence of ρ for LaTiO$_3$e nearly follows T^2 as indicated by the full curve, supporting the fact that this compound is a correlated metal. LaTiO$_3$d1 and d2 are neither simple metals nor semiconductors. They would be defined as poor metals and have small anomalies at about 130 K, which is close to the onset temperature of the cant-magnetism (or spin order) as will be described later. The resistivities of CeTiO$_3$ above 100 K and those of NdTiO$_3$ are both semiconductor-like. The energy gaps E_g/k defined as $\rho = \rho_0 \exp(E_g/kT)$, where ρ_0 is assumed to be a constant and k is the Boltzmann constant, are estimated to be 500 K for CeTiO$_3$ and 1300 K for

$NdTiO_3$, from the full lines in figure 1(*b*). The resistivity data of $LaTiO_3$d1, d2, and $CeTiO_3$ at low temperatures are still small and bend down with decreasing temperature, suggesting the existence of a low-lying excited state. In $PrTiO_3$, the resistivity of about 10 mΩcm depends little on temperature. This may remind us of scattering by impurities [14], where the mean free path of carriers introduced by the excess oxygen (or cation deficiencies) would be comparable to the Ti–Ti distance. Such a behaviour has also been observed in the $Ce_{1-x}Sr_xTiO_3$ system with $0.5 \leqslant x \leqslant 0.9$ [15]. The above results for the nearly stoichiometric and oxygen deficient compounds may be correlated with the change in the bond angle of Ti–O–Ti, such as to reduce the $d\epsilon$–$p\pi$–$d\epsilon$ interactions, or in the bandwidth, with a decrease of the ionic radii of R.

The low-lying excited state in $LaTiO_3$d1, d2, and $CeTiO_3$ is likely to be caused by a slight deviation from the stoichiometric ratio with respect to the atomic concentration and/or by a comparability of the bandwidth and the effective electron–electron correlation energy. Figure 1(*a*) provides a plot based upon a variable-range hopping (VRH) model, $\rho = \rho_0' \exp[(T_0/T)^{1/4}]$, where ρ_0' is a constant and T_0 is equal to α^3/n, α and n representing the envelop of the wavefunction as $\exp(-\alpha r)$ and the density of states for the hopping, respectively [16]. There is no linear relation in a wide temperature region. However, as pointed out above, the anomaly that is probably related to the appearance of the cant-magnetism exists in $LaTiO_3$d1 and d2. The plot for $CeTiO_3$ also suggests the existence of a magnetic transition, but it appears unclear in the semiconductor plot. This may be due to the location of $LaTiO_3$d1, d2, and $CeTiO_3$ near the metal–insulator boundary as described above. Therefore, it is difficult to reach a definite conclusion regarding the transport mechanism from the resistivity results alone. From the VRH viewpoint, the wavefunction of the carriers is expected to extend as the ionic radii of R increase, because T_0 appears to decrease. For $NdTiO_3$, the semiconductor model is considered to be more appropriate than the VRH model, since the correlation energy may be appreciably larger than the bandwidth.

Figure 2 shows the temperature dependence of the thermoelectric power S. In $PrTiO_3$, S is negative, but the others have a positive sign. The large value 10^3 μV K^{-1} of $NdTiO_3$ and its temperature dependence indicate that this compound is a semiconductor and the hole in the lower Hubbard band is responsible for the transport. Except for $NdTiO_3$, S has a tendency to vanish at 0 K. The results of $LaTiO_3$d1, d2, and $CeTiO_3$ are likely to be interpreted as a characteristic of the electron tunnelling between states at the Fermi energy E_F as suggested from the low-temperature behaviour of the resistivity. Since E_F lies in a region where the density of states is finite, the thermoelectric power at low temperatures may be identical to the equation for metallic conduction [17]. The positive sign for $LaTiO_3$d1, d2, and $CeTiO_3$ suggests that the major contribution to the current lies below E_F. At high temperatures, the temperature variation of S is relatively weak, suggesting that the dominant contribution to transport comes by hopping. Therefore, the poor metal phase of $LaTiO_3$d1, d2, and $CeTiO_3$ is defined as a kind of VRH-type insulator.

The result for $PrTiO_3$ may be consistent with the fact that the resistivity is relatively small. By assuming a temperature-independent mean free path of electron carriers, the thermoelectric power is simplified as $S = -(3e)^{-1}\pi^2k^2T/E_F$. From the full line in figure 2, E_F is estimated to be 1900 K.

3.3. Magnetic properties

3.3.1. Paramagnetic susceptibility. The magnetic susceptibility χ of the La compound as a function of temperature is shown in figure 3. In $LaTiO_3$e, χ is relatively small and paramagnetic in the measured temperature region. It decreases with decreasing temperature

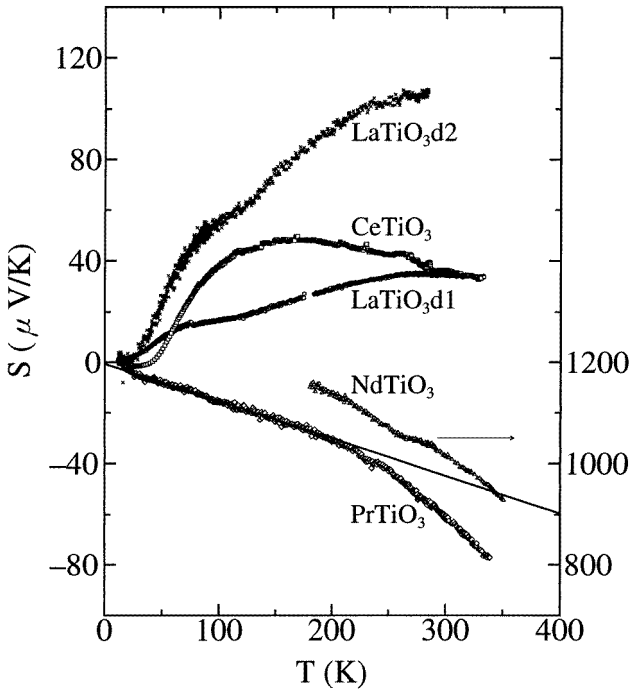

Figure 2. Temperature dependence of the thermoelectric power S of $R\mathrm{TiO_3}$ with R = La, Ce, Pr, and Nd.

above 100 K and then has a slight upturn probably due to a lattice imperfection and/or a magnetic impurity that cannot be detected by standard x-ray powder diffraction. However, $\mathrm{LaTiO_3}$d1 and d2 have sharp susceptibility peaks at $T_c \simeq 126$ K and 138 K, respectively, indicating magnetic transitions. Between T_c and 300 K, χ is nearly constant as reported by several groups [5, 6, 8], but above 300 K it decreases with increasing temperature. Therefore, a clear difference exists between the susceptibilities of $\mathrm{LaTiO_3}$e and $\mathrm{LaTiO_3}$d1, d2. Such a behaviour has also been confirmed in the $\mathrm{La_{1-x}Sr_xTiO_3}$ system [18].

In La compounds, χ is expressed by $\chi = \chi_d + \chi_0$, where χ_d is the d spin susceptibility and χ_0 is the temperature-independent contribution from the Van Vleck paramagnetism and diamagnetism. Using a free-electron relationship, χ_d corresponds to a Pauli paramagnetic susceptibility, $\chi_P = N\mu_B^2(k\mathrm{T})^{-1}F'_{1/2}(\xi)/F_{1/2}(\xi)$, where N and μ_B are the number of electrons and Bohr magneton, respectively, and $F_{1/2}(\xi) = \int x^{1/2}/[\exp(x-\xi)+1]\,\mathrm{d}x$ with $\xi = E_F/kT$ [17]. The full curves in figure 3 are based upon the following parameters of E_F, N, and χ_0: for $\mathrm{LaTiO_3}$d1, 1030 K, 0.96 mol, 2×10^{-5} emu/mol; for $\mathrm{LaTiO_3}$d2, 960 K, 1.02 mol, 2×10^{-5} emu/mol. The contribution from Landau diamagnetism is not significant. The agreement between experimental and calculated results suggests that, even in the VRH-type insulator phase of La compounds, the free-electron model is applied and the Wilson ratio is nearly unity. Therefore, the Wilson ratio in the poor metal phase would be different from the correlated metal phase [8]. However, there exists another possibility that the temperature dependence of a Stoner-type enhancement factor cancels that of the mass enhancement effect, because the present analysis has assumed the latter is constant. In order to clarify this point, further experimental and theoretical works are necessary.

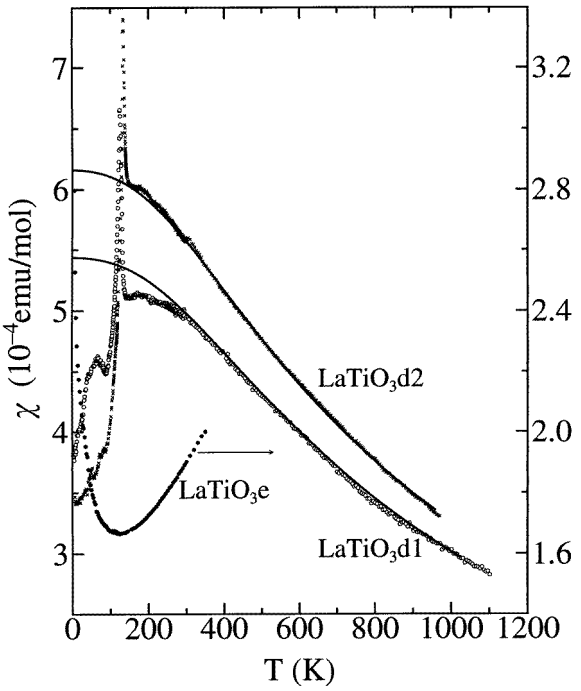

Figure 3. Temperature dependence of the magnetic susceptibility χ of $LaTiO_3$. The full curves are the calculated result from the Fermi-liquid model.

Table 2. Parameters for the magnetic susceptibility and the remanent magnetization of the $RTiO_3$ system.

R	C (emuK/mol)	T_W (K)	χ_0 (emu/mol)	T_c, T_{c1} (K)	σ_0 (μ_B)	H_m (G)	D (K)
La-d1	—	—	—	126	6.0×10^{-3}	—	2.5×10^{-1}
La-d2	—	—	—	138	9.1×10^{-3}	—	4.1×10^{-1}
Ce	0.71(1)	14(3)	$5.8(2) \times 10^{-4}$	124	1.2×10^{-1}	1.1×10^{5}	4.8×10^{0}
Pr	1.44(9)	21(9)	$4.8(28) \times 10^{-4}$	90	1.4×10^{-2}	-6.0×10^{3}	4.2×10^{-1}
Nd	1.51(2)	1.1(9)	$4.4(5) \times 10^{-4}$	107	1.3×10^{-3}	-9.8×10^{2}	4.7×10^{-2}

Although $LaTiO_3$e is a metal, the temperature dependence of χ is clearly different from that of χ_P based on a free-electron relationship. This suggests that the density of states at E_F is not of the form $E^{1/2}$, but has a pseudogap.

The inverse of χ of $CeTiO_3$, $PrTiO_3$ and $NdTiO_3$ as a function of temperature is shown in figure 4. At high temperatures, χ of all the compounds is found to be expressed approximately as a superposition of the Curie–Weiss and constant susceptibilities. The full curves in this figure are based on the Curie constant C, the Weiss temperature T_W, and the constant susceptibility χ_0 listed in table 2. The Curie constants listed in this table are mainly attributed to those of 4f spins of R^{3+} ions. They are approximately 10% smaller than those of free R^{3+} ions due to the crystalline electric field effect. The temperature dependence of χ_d in the Ti^{3+} ions is negligibly small as compared with that of χ_f and may

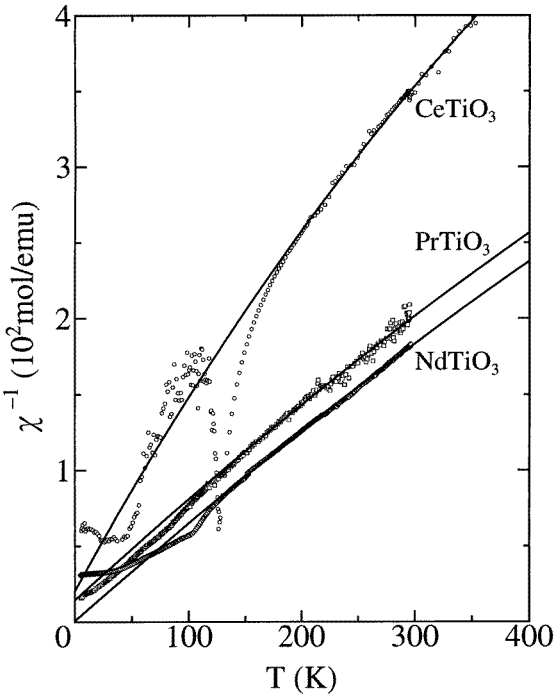

Figure 4. Temperature dependence of the inverse magnetic susceptibility χ^{-1} of $R\mathrm{TiO_3}$ with R = Ce, Pr, and Nd. The full curves are the calculated results from the Curie–Weiss law.

be regarded as a constant, which is consistent with the results below room temperature for La compounds. Thus, χ_0 listed in table 2 contains the contribution from χ_d in the Ti^{3+} ions in addition to those from the Van Vleck paramagnetism and diamagnetism.

The Curie–Weiss law is not valid at low temperatures. In $CeTiO_3$, a sharp peak at $T_{c1} = 124$ K exists and below $T_{c2} \simeq 50$ K, χ becomes almost constant. In $NdTiO_3$, a sharp edge of χ^{-1} and another anomaly appear at $T_{c1} = 107$ K and $T_{c2} \simeq 40$ K, respectively. In the case of $PrTiO_3$, below $T_c \simeq 90$ K, χ becomes larger than the extrapolated value from the high-temperature region. The anomaly at T_c or T_{c1} can be related with the occurrence of the remanent magnetization as will be discussed below.

3.3.2. Cant-magnetism. At T_c or T_{c1} with the susceptibility anomaly, the remanent magnetization σ, defined as $M = \chi H + \sigma$, appears in all the compounds and its temperature dependence is shown in figure 5. As pointed out previously [4], σ in $LaTiO_3$ is considered to originate from the cant-magnetism through an antisymmetric interaction between the Ti^{3+} ions [17, 18]. The temperature dependence of σ_{Ti} is expressed by the relation, $\sigma_{Ti}/\sigma_0 = \tanh[\sigma_{Ti}T_c/(\sigma_0 T)]$, where σ_0 is the value at 0 K. The full curves for $LaTiO_3$d1, d2 in figure 5 provide the values listed in table 2. Here, a slight disagreement between the experimental and calculated results around T_c may be attributed to a short-range ordered effect. In this table, the antisymmetric interaction parameter D is also listed, using the exchange constant J for the d spins estimated through T_c or T_{c1} from the localized electron model for simplicity.

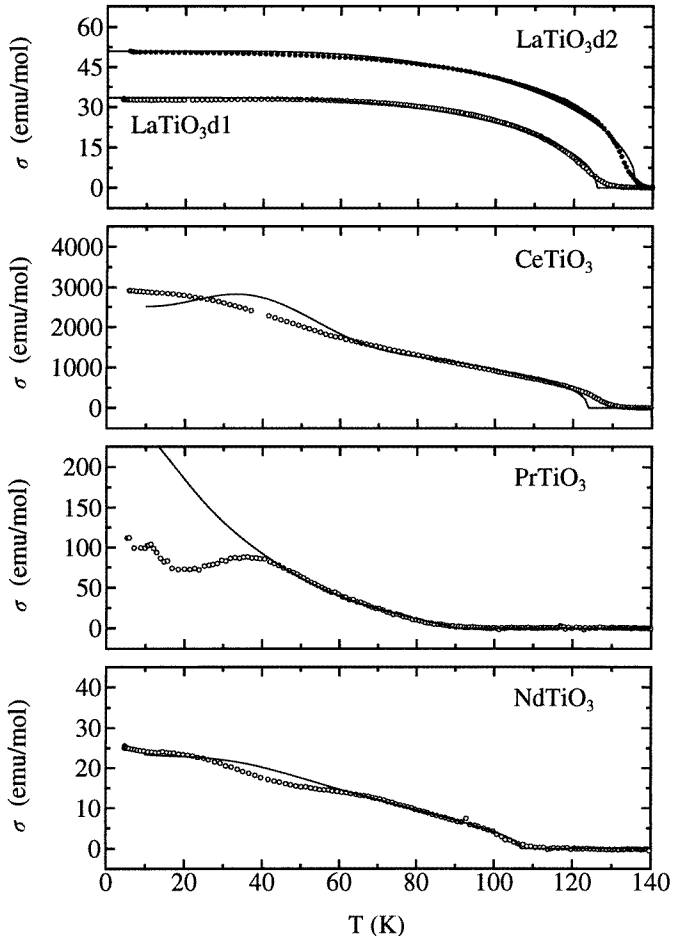

Figure 5. Temperature dependence of the remanent magnetization σ of $R\mathrm{TiO_3}$ with R = La, Ce, Pr, and Nd. The full curves are the calculated results from the antisymmetric interaction and molecular field parameters listed in table 2.

The temperature dependence of σ in $\mathrm{CeTiO_3}$, $\mathrm{PrTiO_3}$, and $\mathrm{NdTiO_3}$ is complex and roughly similar to that in the $R\mathrm{VO_3}$ system [11], where the cant-magnetism originating from the V^{3+} lattice forms the molecular field H_m on the R^{3+} ion. By analogy, σ of $R\mathrm{TiO_3}$ may be expressed as a superposition of σ_Ti and σ_R, these being the cant-magnetism of the Ti^{3+} ion and the magnetization of R^{3+} ion caused via H_m from Ti^{3+}, respectively. The temperature dependence of σ may be calculated from $\sigma = \sigma_\mathrm{Ti}(1 + \sigma_\mathrm{f} H_\mathrm{m})$. Based on σ between T_c ($T_{\mathrm{c}1}$) and $T_\mathrm{c} - 50$ K, the results listed in table 2 and the full curves shown in figure 5 are obtained, where χ_f is assumed to be the same with χ below T_c. In $\mathrm{CeTiO_3}$ and $\mathrm{NdTiO_3}$, the agreement between experimental and calculated results is satisfactory. However, the data below 40 K for $\mathrm{PrTiO_3}$ are not explained, suggesting a change in the canted spin orientation around the R ion. It may also be necessary to consider the effect of magnetic anisotropy.

The onset temperature of cant-magnetism is found to decrease with the decreasing ionic radii of R for the nearly stoichiometric and oxygen deficient compounds. This may be

attributed to the change in the exchange constant between 3d spins, that is, the bond angle of Ti–O–Ti.

The coupling between the canted moment and the 4f spin is found to be ferromagnetic for $CeTiO_3$, but antiferromagnetic for $PrTiO_3$ and $NdTiO_3$. The molecular field on the Ce^{3+} ion is much larger than those of the other ions and comparable to those of the rare-earth iron garnets [19]. The field on the Pr^{3+} and Nd^{3+} ions may correspond to the dipolar field of 3d spins. It is difficult to discuss the origin of H_m in detail without a knowledge of the crystal structures and the canted spin orientation around the R ion at low temperatures. In order to understand the magnetic properties at low temperatures, measurements for single crystals are necessary. The g-shift Δg due to the spin–orbit coupling effect is less than 10^{-1} as found in table 2. This is a reasonable value for $3d^1$ electrons [22].

4. Conclusion

We have studied the electronic states of the $RTiO_3$ (R = La, Ce, Pr, and Nd) perovskite system with Ti^{3+} ions through measurements of x-ray diffraction, transport, and magnetic properties.

The dominant contribution to transport of the nearly stoichiometric and oxygen deficient La and Ce compounds may be by hopping at high temperatures and by extended states at low temperatures due to the existence of a finite density of states at the Fermi level. This is likely to originate from an inhomogeneity in atomic concentration and/or a comparability of the correlation energy and the bandwidth characterized by a change in the transfer integral of the Ti–O–Ti pathway due to TiO_6 tilting. The La and Pr compounds with excess oxygen are metals which may belong to highly- and weakly-correlated regimes, respectively. The Nd compound is a semiconductor due to the relatively small bandwidth.

The oxygen deficient La compounds have a negative temperature derivative of magnetic susceptibility at high temperatures with a large reduction of the Fermi energy, while the compounds with excess oxygen have an anomalous positive value. Thus, the existence of a pseudogap in the density of states is postulated. In $CeTiO_3$, $PrTiO_3$, and $NdTiO_3$, the remanent magnetization at low temperatures is qualitatively understood from the molecular field of the canted moment of Ti ions acting on the 4f spins of R ions. The R dependence of the onset temperature may be correlated with the significant variation in the bandwidth suggested by the transport measurements.

Acknowledgments

We thank Mr T Suganuma for his help in the early stage of our experiments and Professor D S Hirashima for stimulating discussions.

References

[1] Mott N F 1990 *Metal–Insulator Transitions* 2nd edn (London: Taylor and Francis)
[2] Georges A, Kotliar G, Krauth W and Rozenberg M J 1996 *Rev. Mod. Phys.* **68** 13
[3] Bazuev G V, Iutin N N, Matveenko I I and Shveikin G P 1975 *Sov. Phys. Solid State* **17** 747
[4] Greedan J E 1985 *J. Less-Common Metals* **111** 335 and references therein
[5] Lichtenberg F, Widmer D, Bednorz J G, Williams T and Reller A 1991 *Z. Phys.* B **82** 211
[6] Sunstrom J E IV, Kauzlarich S M and Klavins P 1992 *Chem. Mater.* **4** 346
[7] Crandles D A, Timusk T, Garrett J D and Greedan J E 1992 *Physica* C **201** 407
[8] Tokura Y, Taguchi Y, Okada Y, Fujishima Y, Arima T, Kumagai K and Iye Y 1993 *Phys. Rev. Lett.* **70** 2126
[9] Ju H L, Eylem C, Peng J L, Eichhorn B W and Greene R L 1994 *Phys. Rev.* B **49** 13 335

[10] Morikawa K, Mizokawa T, Fujimori A, Taguchi Y and Tokura Y 1996 *Phys. Rev.* B **54** 8446 and references therein
[11] Onoda M and Nagasawa H 1996 *Solid State Commun.* **99** 487
[12] Onoda M, Ohta H and Nagasawa H 1991 *Solid State Commun.* **79** 281
[13] Goodenough J B 1971 *Prog. Solid State Chem.* **5** 145
[14] Ziman J M 1979 *Electrons and Phonons* (Oxford: Oxford University Press)
[15] Onoda M and Yasumoto M 1997 *J. Phys.: Condens. Matter* submitted
[16] Brenig W, Döhler G H and Wölfle P 1973 *Z. Phys.* **258** 381
[17] Wilson A H 1958 *The Theory of Metals* 2nd edn (London: Cambridge University Press)
[18] Onoda M and Kohno M unpublished
[19] Dzyaloshinsky I 1958 *J. Phys. Chem. Solids* **4** 241
[20] Moriya T 1960 *Phys. Rev.* **120** 91
[21] Geller S, Remeika J P, Sherwood R C, Williams H J and Espinosa G P 1965 *Phys. Rev.* **137** A 1034
[22] Abragam A and Bleaney B 1970 *Electron Paramagnetic Resonance of Transition Ions* (Oxford: Oxford University Press)